IOP Publishing Smart Materials and Structures
Smart Mater. Struct. **23** (2014) 104005 (12pp) doi:10.1088/0964-1726/23/10/104005

Wear reduction through piezoelectrically-assisted ultrasonic lubrication

Sheng Dong[1] **and Marcelo J Dapino**[1]

[1] Smart Materials and Structures Laboratory, NSF I/UCRC on Smart Vehicle Concepts, Department of Mechanical and Aerospace Engineering, The Ohio State University, Columbus, Ohio 43210, USA

E-mail: dong.121@osu.edu and dapino.1@osu.edu

Received 3 February 2014, revised 30 March 2014
Accepted for publication 8 April 2014
Published 12 September 2014

Abstract

Traditional lubricants are undesirable in harsh aerospace environments and certain automotive applications. Ultrasonic vibrations can be used to reduce and modulate the effective friction coefficient between two sliding surfaces. This paper investigates the relationship between friction force reduction and wear reduction in ultrasonically lubricated surfaces. A pin-on-disc tribometer is modified through the addition of a piezoelectric transducer which vibrates the pin at 22 kHz in the direction perpendicular to the rotating disc surface. Friction and wear metrics including volume loss, surface roughness, friction forces and apparent stick-slip effects are measured without and with ultrasonic vibrations at three different sliding velocities. SEM imaging and 3D profilometry are used to characterize the wear surfaces and guide model development. Over the range of speeds considered, ultrasonic vibrations reduce the effective friction force up to 62% along with a wear reduction of up to 49%. A simple cube model previously developed to quantify friction force reduction is implemented which describes wear reduction within 15% of the experimental data.

Keywords: piezoelectric, wear reduction, ultrasonic lubrication

1. Introduction

Friction exists when two contacting surfaces slide relative to each other. Material near the surfaces undergo plastic deformation and break away from the body of the material, resulting in surface wear [1]. It has been shown that application of ultrasonic vibrations at the interface of two surfaces in sliding contact reduces the effective friction force between the surfaces [5–13]. This phenomenon, often referred to as ultrasonic lubrication, is promising in applications in which traditional lubrication methods are unfeasible (e.g., vehicle seats, space mechanisms) or where friction modulation is desirable (e.g., automotive steering or suspension components).

Ultrasonic vibrations have been successfully implemented in practical applications. Piezoelectric materials, the transducer elements that typically drive ultrasonic lubrication systems have been incorporated into small control actuators [2], self-levitating sliding contact bearings [3], and industrial components, among others. In metal machining and forming processes such as drilling, pressing, sheet rolling, and wire drawing, ultrasonic vibrations have been utilized to reduce the force between tool and workpiece, leading to improved surface finish [4].

Ultrasonic vibrations are usually applied to only one of the two contacting surfaces. The vibration direction can be perpendicular, longitudinal or transverse relative to the macroscopic sliding velocity. Each of the three directions, and combinations thereof, have been studied. For example, Pohlman and Lehfeldt [5] studied the influence of ultrasonic vibrations on friction between lubricated metal surfaces by applying vibrations in all three directions. They determined that ultrasonic vibrations reduce the internal and external friction force in plastic forming processes. Littman *et al* [6, 7] used a piezoelectric actuator generating vibrations at 60 kHz, making it slide longitudinally on a guide track. Bharadwaj and Dapino [8, 9] also applied longitudinal ultrasonic vibrations to investigate the dependence of friction reduction on macroscopic sliding velocity, normal load, contact stiffness, and global stiffness. Kumar [10] experimentally determined that longitudinal vibrations were more effective at reducing friction force than transverse vibrations and confirmed that the velocity ratio greatly influences the degree of friction reduction.

Popov *et al* [11] studied ultrasonic vibrations for different material combinations. It was shown that ultrasonic vibrations create less friction reduction on softer materials than harder ones. They argued that contact stiffness influences the degree of friction force reduction. Dong and Dapino [12, 13] used the Poisson effect to generate vibrations in combined perpendicular and longitudinal directions and studied the relationship between friction reduction and normal load, contact materials, and global stiffness. An elastic-plastic cube model was proposed to describe ultrasonic friction reduction.

There have been attempts at utilizing vibrations to reduce wear between two contacting surfaces. Chowdhury and Helali [14] developed a pin-on-disc test to examine the effects of micro vibration on wear reduction. Vibrations ranging in frequency from 0 Hz to 500 Hz were applied normal to the disc surface. They studied the correlation between wear reduction and vibration frequency, relative humidity, and sliding velocity. Their results proved that higher frequency leads to lower wear rates. Bryant and York [15, 16] did similar work using high amplitude, low frequency vibrations. They created a slider that vibrates at an amplitude of 10 to 100 μm at frequencies ranging from 10 to 100 Hz, achieving wear reduction of up to 50%.

Goto and Ashida [17, 18] conducted tests at frequencies in the ultrasonic range. Applying vibrations normal to the surface of the disc, they studied the relationship between wear rate and normal loads. Their findings show that ultrasonic vibrations can reduce wear under various normal loads. In these tests, the amplitude of the ultrasonic vibrations was 8 μm and the normal load was up to 88 N. They also studied the contact time between two surfaces while ultrasonic vibrations were applied.

It has been shown that linear speed plays an important role in the performance of ultrasonic lubrication. However, the influence of linear speed on wear reduction is not well documented. Therefore, this paper focuses on the relationship between friction and wear reduction at various linear speeds.

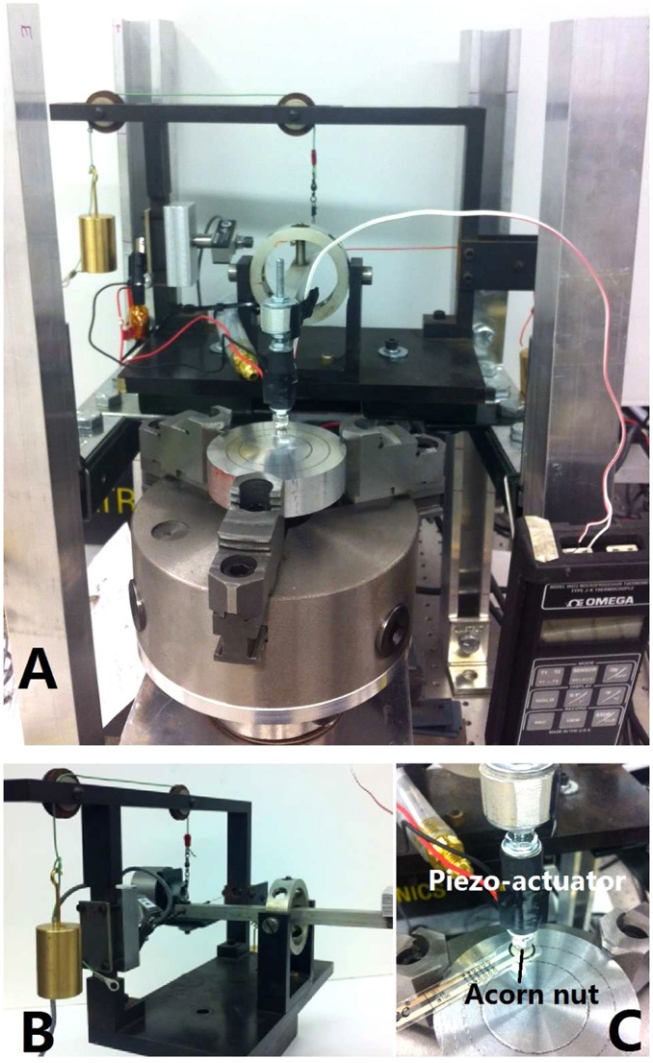

Figure 1. Experimental set-up: (A) overall tribometer; (B) detailed gymbal assembly; and (C) piezoelectric actuator.

2. Experiments

2.1. Set-up

The experimental set-up used in this study is a modified pin-on-disc tribometer, as shown in figure 1(a). This tribometer applies a specified force between a still pin and a rotating disc for the purpose of studying the characteristics of friction and wear on the disc surface. The pin has been modified with the addition of a piezoelectric actuator and an acorn nut with a rounded end (figure 1(c)). The actuator imparts ultrasonic vibrations to the rotating disc along the direction perpendicular to the disc. The pin is held by a lever which is part of a gymbal assembly that has been installed on the frame (figure 1(b)). Weights connected to the gymbal assembly apply a force normal to the surface of the disc. The normal force is measured by a load sensor pad placed between the pin and the disc. The resistance of the sensor pad changes as a function of the applied force, resulting in a change of output voltage. The gymbal assembly is instrumented to measure friction forces using a load cell. The load cell is installed on one side of the assembly frame and pretensioned horizontally by a weight located on the other side. A schematic is shown in figure 2.

The piezoelectric actuator generates vibrations with amplitude of 2.5 μm at a frequency of 22 kHz. The temperature of the actuator can increase rapidly from the heat generated and accumulated during the test. To maintain even temperatures, air flow and a thermocouple are employed to cool down the actuator and monitor the temperature, respectively. The disc is 76.2 mm (3 in.) in diameter and held in place by a lathe chuck. The chuck, which is placed on a platform, is driven by a DC motor and variable speed controller.

2.2. Parameters and schematics

Three groups of tests were conducted at linear speeds of 20.3, 40.6, and 87 mm s^{-1}. The distance traveled by the pin and the

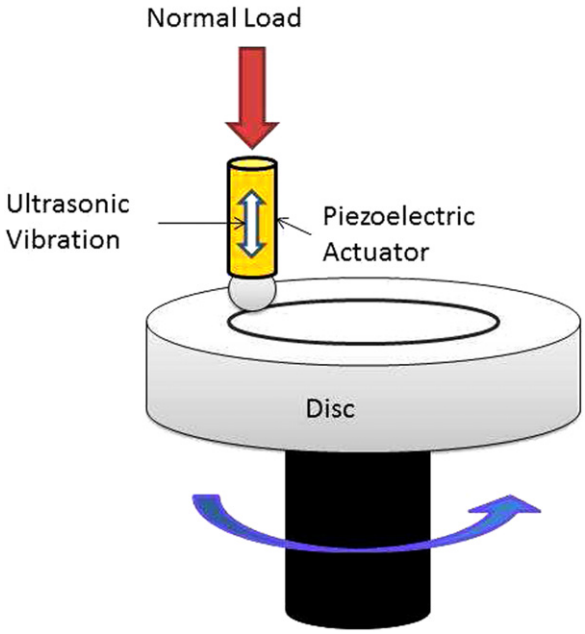

Figure 2. Schematic of modified pin-on-disc tribometer.

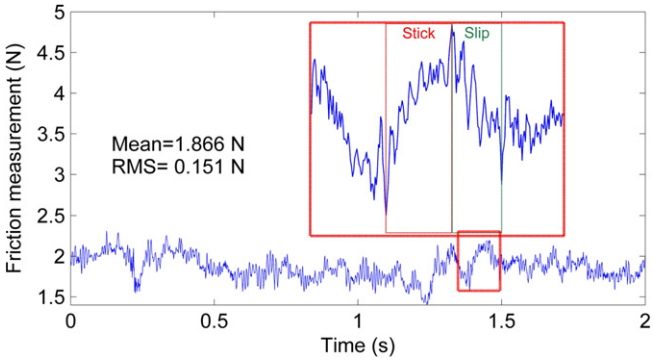

Figure 3. Time trace of the measured friction force showing the stick-slip effect.

Table 1. Parameters utilized in the tribometer tests.

Parameter	Value		
Linear speed $\left(\text{mm s}^{-1}\right)$	20.3	40.6	87
Running time (h)	4	2	0.93
Distance traveled by pin (m)	292.5		
Revolutions	1600		
Pin material	Stainless steel 316		
Disc material	Aluminum 2024		
Nominal normal force (N)	3		
Disc runout (mm)	±0.0286		
US frequency (kHz)	22		
US amplitude (μm)	2.5		
Nominal Groove diameter (mm)	50		
Nominal temperature (°C)	21 ± 1		
Nominal actuator temperature (°C)	31 ± 1		
Environment	Laboratory air		
Sampling frequency (Hz)	400		

number of revolutions were kept constant by changing the duration of the test. For each speed, tests were conducted with and without ultrasonic vibrations. The remaining test parameters were fixed as shown in table 1.

Friction force was sampled at a frequency of 400 Hz and each sampling window was 2 s. Typical data from a single sampling window appears in figure 3. The observed fluctuation in friction force is attributed to stick-slip. The mean value and root mean square (RMS) value of the variation were calculated for each sampling window. A profilometer was then employed to measure the volume loss of the discs and the roughness parameters of the disc surfaces.

2.3. Procedures

Each pin-on-disc test was conducted following the procedures suggested by ASTM G99 [19] with modifications:

(a) Clean and dry the acorn nut and disc specimens immediately prior to testing. Ethanol and acetone were used to remove all foreign matter.
(b) Insert the sample securely into the chuck so that the disc is perpendicular to the axis of revolution in order to minimize wobbling.
(c) Install the acorn nut and compress it tightly against the piezoelectric actuator.
(d) Adjust the position of the pin, making sure that it is perpendicular to the disc surface.
(e) Add weight for application of normal loads.
(f) Start the motor and adjust the speed to the desired value while preventing the pin from making contact with the disc, then stop the motor.
(g) Record the temperature and ambient environment of the tests. Prepare the data acquisition system for testing.
(h) Put the pin in contact with the disc. Start the motor and the piezoelectric actuator (when applicable). Stop the motor when the desired running time is reached.
(i) Clean the specimens and measure the volume loss and roughness parameters using a profilometer.

3. Results and discussion

3.1. Friction without ultrasonic vibrations

Mean friction values for three linear speeds are plotted against pin travel distance in figure 4. In each case, the friction force increases rapidly initially, reaches steady state after a certain travel distance, and remains at that level for the remainder of the test. There is fluctuation of friction force after it reaches steady state. Unlike the fluctuation observed in figure 3, which is due to stick-slip, the fluctuation here is caused by disc runout. The disc wobbles a small amount while rotating. The inertia from the up and down pin movement causes fluctuation of the normal force, and accordingly, fluctuation of the tangential friction force.

Table 2 lists the steady state friction forces, their RMS values and the stabilization distance. As expected, the

Table 2. Steady state friction forces and distances to achieve steady state.

Linear speed $\left(\text{mm s}^{-1}\right)$	US	Steady state friction (N)	Distance to achieve steady state (m)	RMS of steady state friction (N)	Distance to achieve steady state (m)
20.3	No	1.024 ± 0.063	4.17	0.197 ± 0.039	3.11
	Yes	0.379 ± 0.041	2.78	0.081 ± 0.020	35.71
40.6	No	1.201 ± 0.055	11.61	0.251 ± 0.034	7.97
	Yes	0.748 ± 0.035	7.21	0.096 ± 0.033	45.44
87	No	1.472 ± 0.064	8.94	0.249 ± 0.033	3.22
	Yes	1.041 ± 0.056	4.64	0.188 ± 0.021	31.53

intrinsic friction force (force without ultrasonic vibrations) increases as the speeds increase. For metals, the friction-speed curve has a positive slope when speeds are low and a negative slope when speeds are high [20–22]. The speeds adopted in this study are relatively low.

3.2. Friction reduction

The mean value of the measured friction force with applied ultrasonic vibrations is plotted versus sliding distance in figure 5 for three linear speeds. As with the intrinsic friction force, the measurement in each of these cases reaches steady state after the pin has traveled a certain distance over the surface of the disc. As in the previous case, the friction force fluctuates because of disc runout. However, the fluctuation amplitudes are smaller because the inertial forces on the pin are reduced when ultrasonic vibrations are present.

The friction reduction percentage is defined as

$$P_f = \frac{f_0 - f_1}{f_0} \times 100, \tag{1}$$

where f_0 is the intrinsic friction force and f_1 is the friction force when ultrasonic vibrations are applied. The friction reduction percentages for each linear speed are plotted in figure 6. All three linear speeds give consistent friction reduction at steady state; a lower sliding speed results in greater friction force reduction.

Table 2 lists the steady-state friction forces, their RMS values, and the distances needed to reach steady state. As is the case with the intrinsic friction force, the friction force when ultrasonic vibrations are applied increases as the linear speed increases. The trend is shown in figure 7, where the markers indicate the mean values and the error bars are the RMS of the steady state values.

It is emphasized that it takes a shorter distance for the force to stabilize when ultrasonic vibrations are applied, for the three linear speeds tested. The ultrasonic vibrations make it easier for the oxide layer of the pin and disc to break down and build up a steady contact while it takes a longer time for that to occur without ultrasonic vibrations. At the intermediate speed $\left(40.6\ \text{mm s}^{-1}\right)$ the force takes longer to stabilize both with and without ultrasonic vibrations.

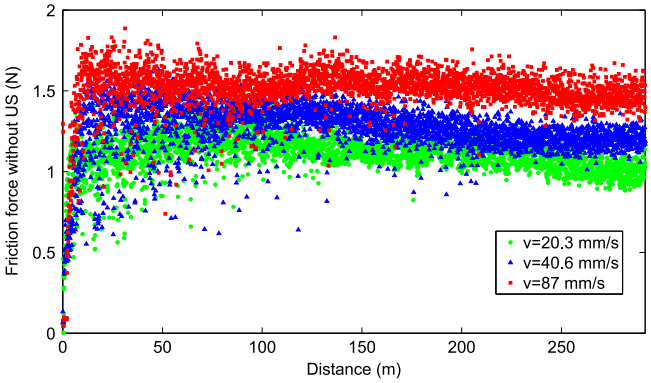

Figure 4. Measured friction forces without ultrasonic vibrations.

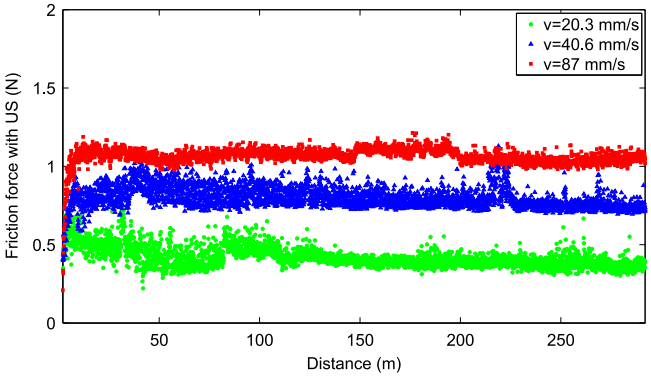

Figure 5. Measured friction forces with ultrasonic vibrations.

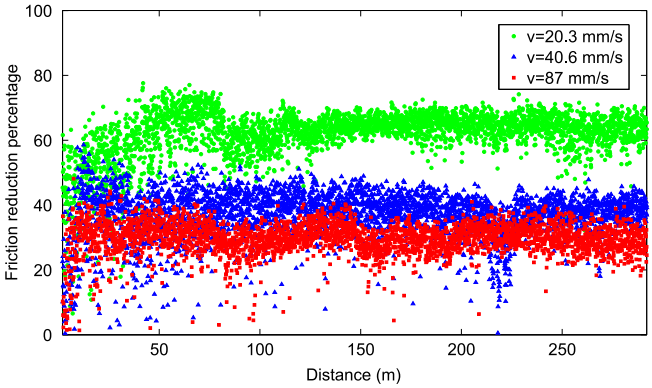

Figure 6. Measured friction reduction calculated from (1).

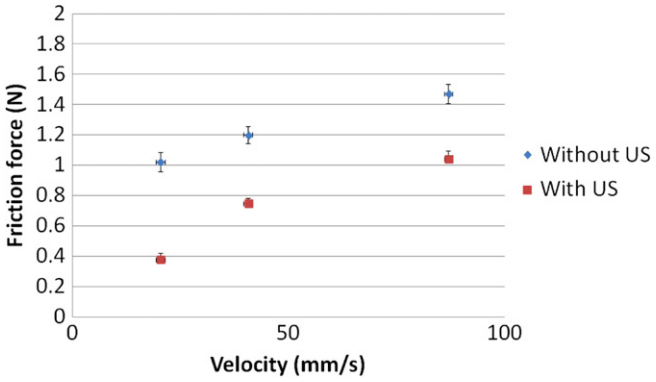

Figure 7. Relationship between measured friction force and linear speed.

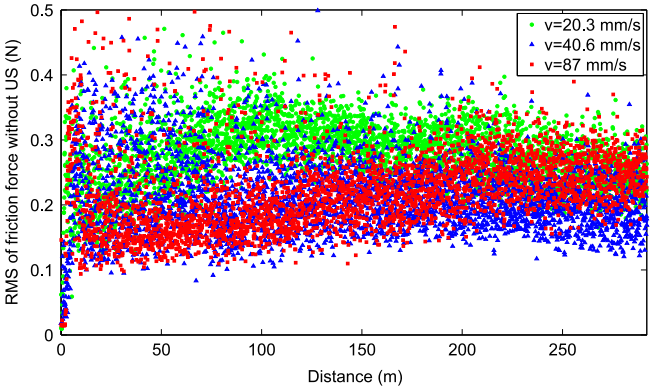

Figure 8. RMS of friction force without ultrasonic vibrations.

3.3. RMS of friction force variation

As shown in figure 3 (inset), the instantaneous friction force fluctuates due to stick-slip. Stick is the stage when two objects stay relatively still and friction increases. Slip happens when the friction increases to such an extent that the two surfaces release to slide relative to each other. A commonly accepted explanation for stick-slip is that the effective friction coefficient varies during sliding over a range covering the static and dynamic coefficients [22]. Another cause of stick-slip can be the waviness of the surface, which results in an inconsistent effective friction coefficient [20]. In this study, the average amplitude of the stick-slip fluctuation is found from the RMS value of the measured force. This calculation is performed over consecutive 2-second boxcar windows. The RMS friction force is plotted versus travel distance for each of the tests groups without ultrasonic vibrations (figure 8) and with ultrasonic vibrations (figure 9).

In both cases, the RMS values reach steady state after a certain distance is reached. Contrary to the mean values, however, it takes significantly longer for the stick-slip to stabilize when the ultrasonic vibrations are on than when they are off. The stick-slip amplitudes are nearly the same for the three speeds when the ultrasonic vibrations are absent. When the vibrations are applied, all three cases show amplitude reductions with different levels. The steady state values of friction force and distances to achieve steady state friction are presented in table 2; figure 10 shows the RMS value of friction force with the markers indicating the average value of the RMS force over the entire test and the error bars represent one standard deviation of the RMS values.

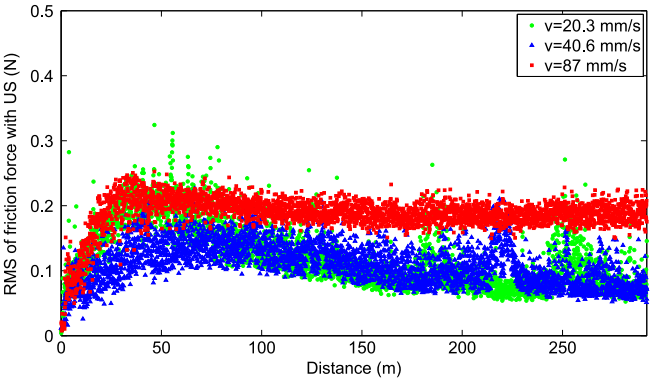

Figure 9. RMS of friction force when ultrasonic vibrations are applied.

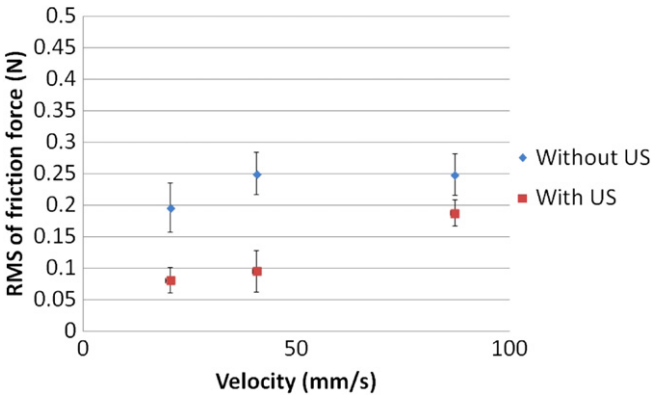

Figure 10. Relationship between RMS of friction force and linear speed.

3.4. Wear reduction

The materials in this study, stainless steel and aluminum, exhibit hardnesses ranging from 700 to 950 kg mm^{-2} and from 45 to 50 kg mm^{-2}, respectively. Due to the difference in hardness, the type of wear between them is abrasive: the harder material digs into the softer one, removing material and creating grooves [23].

Images of the wear grooves from all test groups are shown in figure 11. Each image shows approximately one quarter of the whole groove. It can be observed that the grooves from tests with ultrasonic vibrations (images A, C, E) appear more uneven and non-reflective than the ones without it (images B, D, F).

A 3D profilometer was employed to quantify the wear volume loss and obtain the profiles of the wear grooves along with roughness parameters of the scanned surface. Eight spots along the path of each wear ring were scanned. Each scan was conducted over an area of 1.8 mm by 2.4 mm with a scan stroke of ±100 μm. The 3D profiles of the grooves from all

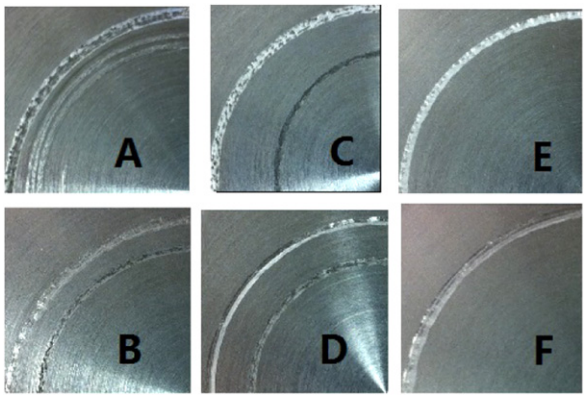

Figure 11. Wear grooves obtained with ultrasonic vibrations (A, C, and E) and without ultrasonic vibrations (B, D, and F). Each column corresponds to a linear speed: 20.3 mm s^{-1} (A, B); 40.6 mm s^{-1} (C, D); and 87 mm s^{-1} (E, F).

linear speeds are shown in figure 12. The groove topology changes when ultrasonic vibrations are applied by becoming narrower and less smooth. This explains why the grooves appear uneven in figure 11. Round dents are observed in B, D and F, becoming more distinct as linear speed increases. This effect is not observed without ultrasonic vibrations. The color coding representing the depth of the grooves shows that the grooves are shallower when ultrasonic vibrations are applied. In addition, the surface roughness parameters are consistently lower when ultrasonic vibrations are applied, as shown in table 3. In combination, these measurements suggest that ultrasonic vibrations reduce wear.

To quantify the degree of wear reduction, wear rate is defined as

$$W = \frac{V}{D}, \tag{2}$$

where V is disc volume loss in mm^3 and D is the distance travelled by the pin in meters. The disc volume loss is calculated from data of groove volume obtained with the

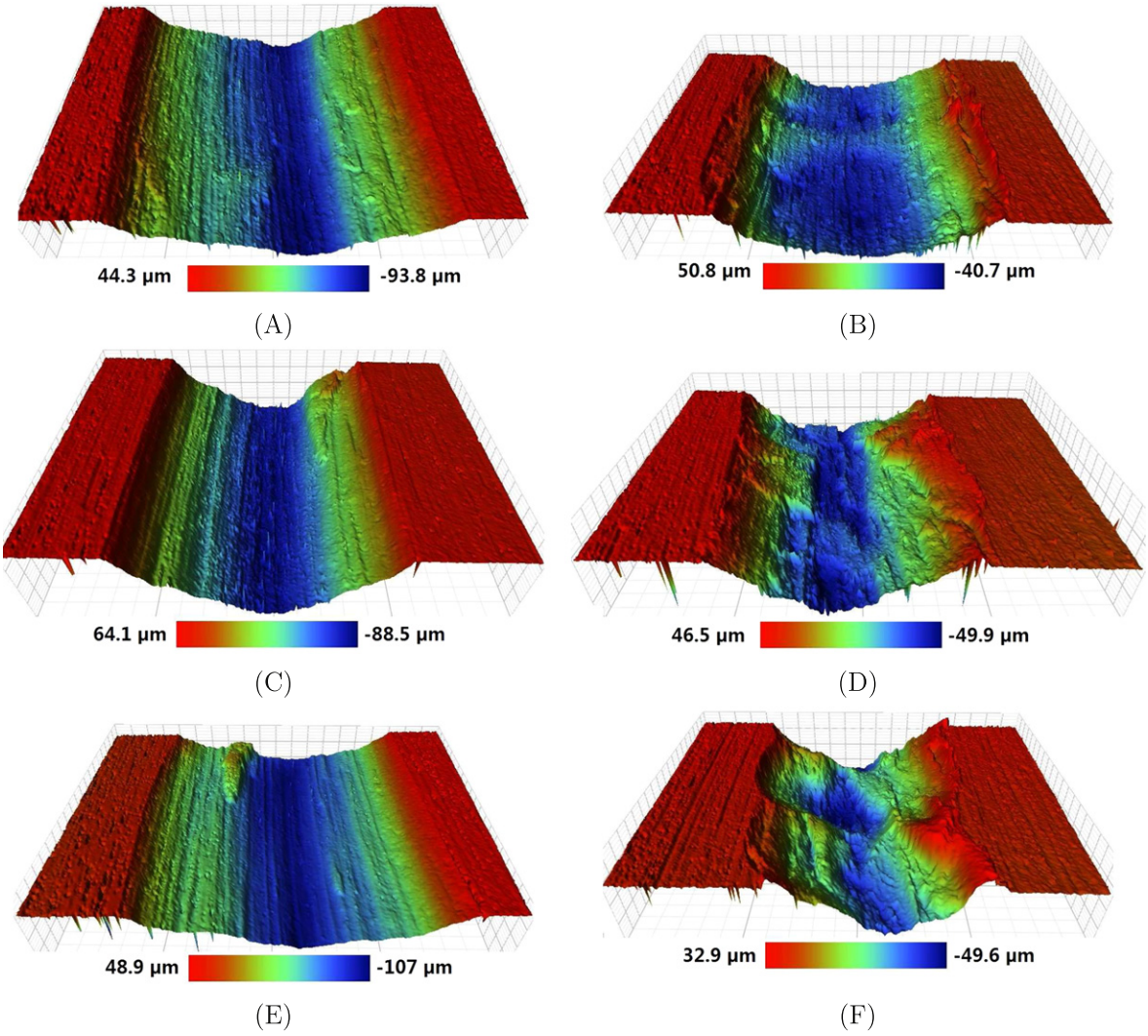

Figure 12. 3D profiles of wear grooves obtained without ultrasonic vibrations (A, C, E) and with ultrasonic vibrations (B, D, F). Each row represents a linear speed: 20.3 mm s^{-1} (A, B); 40.6 mm s^{-1} (C, D); and 87 mm s^{-1} (E, F).

Table 3. Comparison of surface roughness parameters: R_a arithmetic average; R_p maximum peak height; R_q root mean squared; R_t maximum height of the profile; and R_v maximum valley depth.

Speed $\left(\text{mm s}^{-1}\right)$	US	R_a (μm)	R_p (μm)	R_q (μm)	R_t (μm)	R_v (μm)
No wear		0.45	10.071	0.58	18.887	8.816
20.3	N	18.829	48.440	21.421	124.35	75.906
	Y	17.238	38.458	18.975	87.011	48.554
40.6	N	21.647	46.646	22.673	109.28	62.638
	Y	17.289	42.469	19.922	106.42	63.947
87	N	19.825	48.910	21.921	130.52	81.612
	Y	17.606	44.245	20.126	111.25	66.877

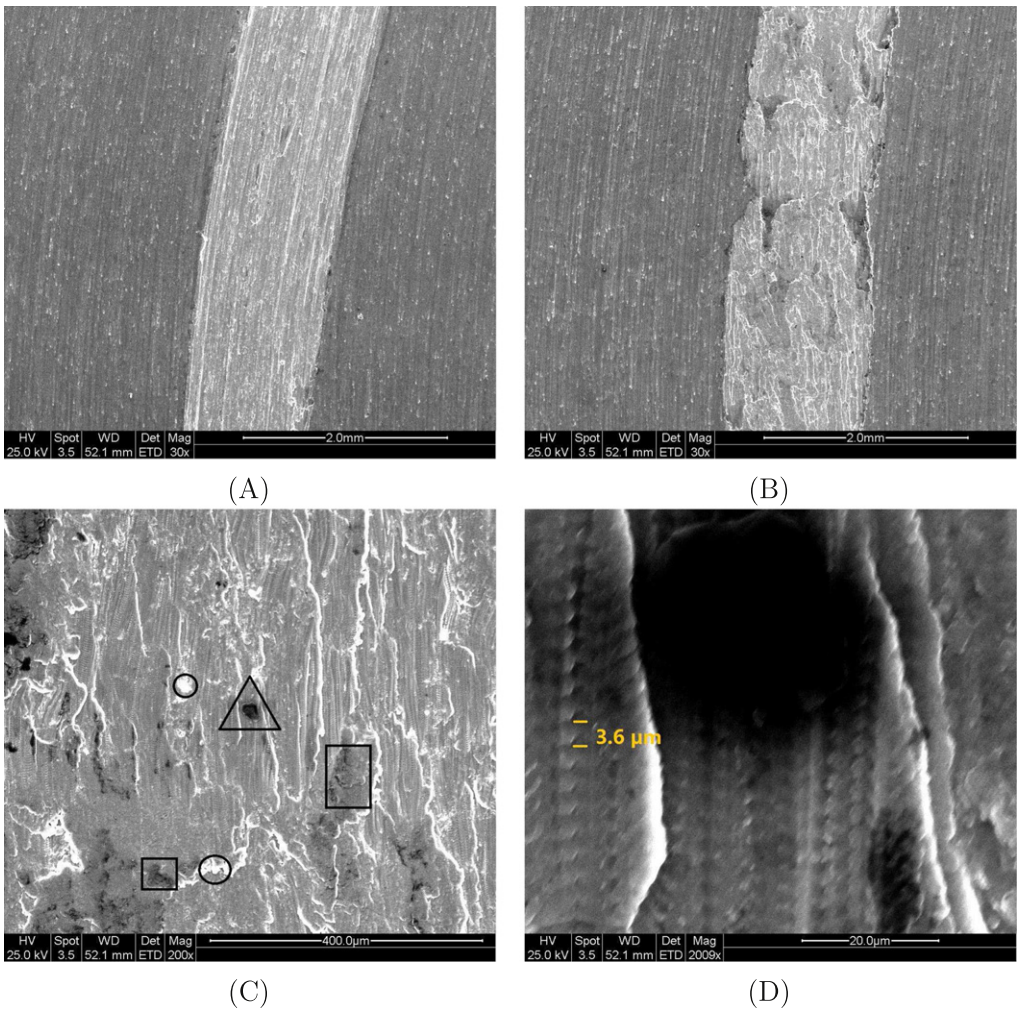

Figure 13. SEM images of wear grooves: (A) without ultrasonic vibrations, and (B) with ultrasonic vibrations. Image (C) is a close-up of (B), whereas further magnification of the same image is shown in (D).

profilometer. The wear reduction percentage is defined as

$$P_w = \frac{W_0 - W_1}{W_0} \times 100, \tag{3}$$

where W_0 is the wear rate without ultrasonic vibrations applied and W_1 is the wear rate with ultrasonic vibrations applied. The wear rates and wear reduction percentages are listed in table 4. The results show that the wear rate is nearly constant for the three linear speeds, both with and without ultrasonic vibrations. The wear reduction percentage slightly increases as the speed increases. Few previous studies focused on the relationship between abrasive wear and sliding speed, but the effect of sliding distance on friction has been investigated in depth [24, 25]. Studies have shown that when there is unlimited abrasive material (harder material), the wear rate is initially low and subsequently increases until it reaches a steady state value. However, if the abrasive material is limited, the wear rate will decrease as the test continues. In both

cases, the wear rate was found not to depend on the sliding velocity.

There is a close correlation between the observed stick-slip and the topology of the grooves. The segment of the groove in figure 12(F) shows two indentations which were created by the contact between pin and disc during the stick phase. The measured distance between the two indentations is 0.869 mm. It is noted that the scale on the plane of the surface is different than the scale along the depth direction. The distance between the indentation centers can be estimated by

$$s = \Delta t \times v, \tag{4}$$

where $\Delta t = 0.01$ s is the period of stick-slip (high frequency component in the inset of figure 3) and v is the linear speed. The calculated distances are 0.213 mm, 0.426 mm, and 0.853 mm for the three linear speeds of 20.3 mm s^{-1}, 40.6 mm s^{-1}, and 87 mm s^{-1}, respectively. The data and calculation match well for the speed of 87 mm s^{-1}. However, the individual indentations are not as evident in the other two cases because at these lower speeds the indentations overlap one another. When no ultrasonic vibrations are applied, the pin and disc make contact during both the stick and slip phases, creating little waviness along the grooves.

Scanning electron microscopy was employed to observe in detail various wear features and quantify key dimensions of wear patterns. Images (A) and (B) in figure 13 were taken of the grooves created without and with ultrasonic vibrations at a speed of 87 mm s^{-1}, respectively. The wear pattern without ultrasonic vibrations shows a uniform shade of gray and straight white lines, while the one with ultrasonic vibrations has curved white lines and various darker irregularities. Image (C) shows a magnified view of the groove in image (B). The groove surface includes voids (black), deposits of foreign materials from the pin (gray), and oxide layers (white), which are marked with triangular, rectangular, and circular shapes, respectively. The white dotted lines are the traces of the contact points between pin and disc asperities. Image (D) shows a close-up of those lines. The visible white dots are attributed to a punching action of the pin on the disc as the piezoelectric actuator cyclically increases and decreases the contact pressure between the two. The nominal distance between the dots is measured as 3.6 μm, which is close to the value of 3.9 μm calculated from the ratio of linear speed and frequency of ultrasonic vibrations. It is proposed that the contact between the pin and disc takes place only on groups of asperities instead of the whole nominal area of contact. This observation motivates one of the assumptions made to develop the cube model for wear, explained in the following section.

3.5. Discussion

The measurements indicate that ultrasonic vibrations are effective in reducing friction, stick-slip, and wear at all three linear speeds (see figure 14).

With increasing speed, the degree of friction reduction decreases from 62.2% for 20.3 mm s^{-1} to 29.3% for 87 mm s^{-1}. A similar observation was reported by Littmann *et al* [6], who studied the relationship between velocity ratio and friction ratio by applying ultrasonic vibrations along the direction of the macroscopic speed. In their study, the velocity ratio was defined as the macroscopic velocity over the propagation speed of the ultrasonic waves. The friction ratio was defined as the friction force with ultrasonic vibrations over friction force without ultrasonic vibrations. It was proposed that a small velocity ratio leads to a low friction ratio, and hence effective friction reduction. As the velocity ratio increases, so does the friction ratio until a value of 1 is achieved and no further benefit from the ultrasonic vibrations is possible. Therefore, an increase in sliding velocity moves the system towards a friction ration of 1 and reduces the effectiveness of the ultrasonic vibrations. Conversely, to maintain high friction reduction for high sliding velocities, a high vibration frequency is necessary. Due to the nature of piezoelectricity, achieving high frequency of operation requires an actuator capable of high output power.

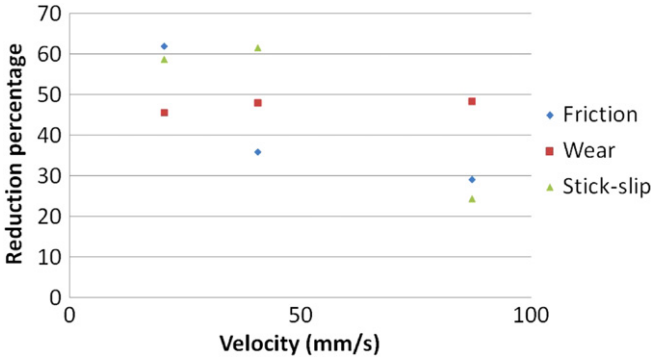

Figure 14. Relationship between reduction results and linear speeds.

Pohlman and Lehfeldt [5] conducted similar ball-on-disc experiments by applying ultrasonic vibrations collinear, transverse, and normal to the macroscopic sliding velocity. Molykote was used to lubricate the interface. In those experiments, ultrasonic vibrations change the lubrication regime by changing the relative sliding velocity. They achieved friction reduction by applying the vibrations in-plane (tangential and transverse) because that is the most effective way to change the relative velocity. In our experiments, ultrasonic vibrations change the contact stiffness. We achieve friction reduction when applying the vibrations normal to the disc because it is effective to change the contact stiffness that way. Pohlman and Lehfeldt did not achieve friction reduction in the normal direction because the lubricant prevents an intimate contact between the two surfaces, which leads to little or no change in the contact stiffness when ultrasonic vibrations are applied.

In our measurements, wear reduction varies over a narrow range with changing linear speed (45.8%–48.6%). Surprisingly, a higher velocity results in a slightly higher wear reduction. One explanation is that as speed increases the actual contact between the pin and the disc decreases. Studies showed that when the amplitude of ultrasonic vibrations is large enough, the contact time between two sliding surfaces is

Table 4. Reduction percentages as a function of linear speed for friction force, wear, and stick-slip measurements.

Linear speed $\left(\text{mm s}^{-1}\right)$	Wear rate without US ($\text{mm}^3\ \text{m}^{-1}$)	Wear rate with US ($\text{mm}^3\ \text{m}^{-1}$)	Wear reduction ($\text{mm}^3\ \text{m}^{-1}$)	Wear reduction (%)	Number of contacts	Friction reduction (%)
20.3	2.237×10^{-2}	1.214×10^{-2}	1.023×10^{-2}	45.76	3.17×10^{8}	62.22
40.6	2.581×10^{-2}	1.338×10^{-2}	1.243×10^{-2}	48.18	1.58×10^{8}	36.11
87	2.430×10^{-2}	1.248×10^{-2}	1.182×10^{-2}	48.63	7.39×10^{7}	29.32

reduced as one surface moves away from the other [17, 18]. Assuming that the pin makes one contact with the disc and then moves away from it in one cycle of ultrasonic vibration, the number of contacts between the disc and the pin over the duration of a test can therefore be estimated. These values are presented in table 4.

The relationship between stick-slip reduction and linear speed does not follow the same trend. As shown in figure 14, the percentage reduction of stick-slip first increases with linear speed and then decreases. It has been shown that the amplitude of vibration caused by stick-slip is related to the stiffness and damping of the system and that increasing the stiffness can greatly reduce the amplitude of vibration [20]. The reason is that stick-slip can be considered as an excitation to the system, and linear speeds in addition to the waviness of the surface can change the frequency of the excitation. At certain speeds, the system is excited at its resonance frequency, which results in a magnification of the stick-slip vibration. The system resonance frequency can be increased if the system is stiffer. Therefore, the possibility of magnifying the vibration is reduced when the surfaces slide at the same range of speeds [26].

4. Cube model for wear reduction

A 'cube' model was initially proposed by Dong and Dapino [13] for ultrasonic friction reduction. The model is built on the assumption that the contact between two surfaces sliding relative to each other takes place only on the asperities, which deform elastically and plastically. The height of the asperities is assumed to follow the distribution

$$\phi(z) = ce^{-\lambda z}, \tag{5}$$

where z is the distance between the asperity summit and the mean height of asperities. Here, $c = 17$ and $\lambda = 3$ are parameters used to shape the distribution [27].

A cube is employed to represent the asperities in contact. The height of the cube d is equal to the distance between the two surfaces in contact. The normal force F_n is the sum of the elastic force F_e and the plastic force F_p, which are functions of d,

$$F_n = F_e + F_p. \tag{6}$$

The cube height d corresponding to a normal load F_n is calculated using [13]

$$F_e = \frac{4c\beta A_n E^*\left(R_q/R_s\right)^{1/2}}{3\lambda^{5/2}}\left[\frac{3\sqrt{\pi}}{4}\,\text{erf}\left(\sqrt{\lambda\omega_c/R_q}\right) - \frac{\left(\lambda\omega_c/R_q\right)^{3/2} + \frac{3}{2}\sqrt{\lambda\omega_c/R_q}}{e^{\lambda\omega_c/R_q}}\right]e^{-\lambda d/R_q} \tag{7}$$

and

$$F_p = \frac{cA_n\pi\beta C_\nu\left(1-\nu^2\right)Y_0}{\lambda^2}\left(2+\lambda\frac{\omega_c}{R_q}\right)e^{-\lambda\left(d+\omega_c\right)/R_q}, \tag{8}$$

where β is the roughness parameter ($\beta = \eta R_q R_s$), η is the areal density of asperities, A_n is the nominal contact area, R_q is the standard deviation of surface roughness, R_s is the average radius of asperity summits, ν is the Poisson ratio, erf is the error fuction $\left(\text{erf}(x) = \frac{2}{\sqrt{\pi}}\int_0^x e^{-t^2}dt\right)$, C_ν is a hardness coefficient ($C_\nu = 1.234 + 1.256\nu$), Y_0 is the failure strength of the softer material, and E^* is the combined Young's modulus of the two materials in contact $\left(1/E^* = \left(1-\nu_1^2\right)/E_1 + \left(1-\nu_2^2\right)/E_2\right)$. Parameter ω_c is the critical interference, defined as the threshold asperity height separating elastic and plastic deformations, which is calculated as

$$\omega_c = \left[\frac{C_\nu\pi\left(1-\nu^2\right)Y_0}{2E^*}\right]^2 R_s. \tag{9}$$

The top area of the cube is equal to the actual contact area between the two surfaces:

$$A_r = A_e + A_p, \tag{10}$$

where A_e is the actual contact area of elastically deformed asperities and A_p is that of the plastically deformed asperities. These areas are given by [13]

$$A_e = \frac{c\pi\beta A_n}{\lambda^2}\left[1-\left(1+\lambda\frac{\omega_c}{R_q}\right)e^{\lambda\omega_c/R_q}\right]e^{-\lambda d/R_q}, \tag{11}$$

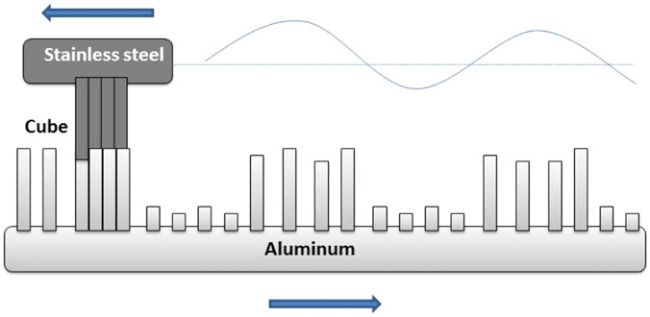

Figure 15. Mechanics of ultrasonically-induced wear reduction.

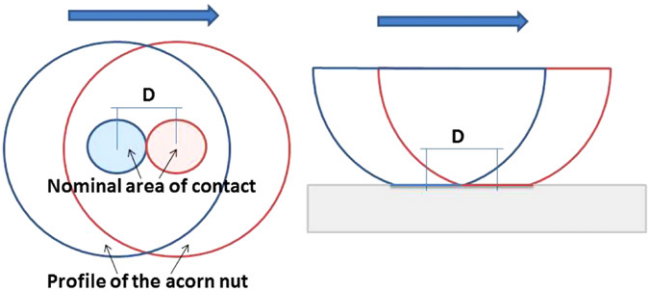

Figure 16. Schematic of wear rate calculation.

and

$$A_p = \frac{c\pi\beta A_n}{\lambda^2}\left(2 + \lambda\frac{\omega_c}{R_q}\right)e^{-\lambda\left(d+\omega_c\right)/R_q}, \tag{12}$$

Based on the cube concept, a description for ultrasonic wear reduction is proposed. It can be seen in figure 15 that as the top surface moves along the bottom surface, contact asperity pairs deform and break, bringing new asperities into contact. As addressed previously, wear in this study is abrasive in nature due to the fact that stainless steel is much harder than aluminum. Breakage of the contacting asperity pairs is assumed to take place at the roots of the asperities of the softer material, i.e. the aluminum disc. The broken asperities correspond to half of the cube's volume; this removed volume accounts for abrasive wear in the aluminum disc. When ultrasonic vibrations are applied, the contact between the two surfaces is reduced resulting in a reduction of wear.

An approach to quantify wear reduction is illustrated in figure 16. The geometry considered is that of the stainless steel acorn nut used in the experiments as it slides relative to the aluminum disc. Over the sliding distance D, the total volume of material removed is calculated as

$$V = \frac{A_r d}{2}, \tag{13}$$

where V is the volume loss of the aluminum disc, A_r is the actual area of contact between the two surfaces, and d is the height of the cube. Distance D can be calculated from the nominal area A_n as

$$D = \frac{4\sqrt{A_n}}{\pi}. \tag{14}$$

When ultrasonic vibrations are applied, the acorn nut vibrates in the direction perpendicular to the disc surface. The contact area and the separation between the two surfaces change accordingly. We denote A_r' the area of the top of the cube and d' the height of the cube when ultrasonic vibrations are applied. The volume loss of the aluminum disc over the sliding distance D is

$$V' = \frac{1}{2T}\int_0^T A_r' \mathrm{d}'\mathrm{d}t, \tag{15}$$

where T is the period of ultrasonic vibrations, A_r' is the time-dependent actual area of contact when ultrasonic vibrations are applied, and d' is the time-dependent height of the cube. The wear rate is calculated as

$$W' = \frac{V'}{D} = \frac{1}{2T}\int_0^T \frac{A_r' \mathrm{d}'}{D}\mathrm{d}t, \tag{16}$$

The parameters used to perform these calculates are listed in table 5.

A comparison between the experimental data and the model calculations with and without ultrasonic vibrations is shown in table 6. The calculation errors are consistently smaller than 15%.

Table 5. Parameters used in the cube model for wear reduction.

Symbol	Meaning	Value
F_n	Normal force	3 N
E^*	Combined Young's modulus	59.6 GPa
A_n	Nominal contact area	2.25 mm^2
R_q	RMS of asperity heights	6 μm
R_s	Summit radius of single asperity	1.5 μm
η	Areal density of asperities	4.7×10^{10} m^{-2}
Y_0	Yield strength of softer material	410 MPa

5. Concluding remarks

In this study, a modified pin-on-disc tribometer was built for investigating the effect of ultrasonic vibrations on friction and abrasive wear between stainless steel pins and aluminum discs under a normal load of 3 N. Ultrasonic vibrations generated by a piezoelectric actuator had an amplitude of 2.5 μm and a frequency of 22 kHz. Three different linear speed were considered (20.3 mm s^{-1}, 40.6 mm s^{-1}, and 87 mm s^{-1}) while keeping other parameters unchanged throughout the testing.

The friction measurements show that ultrasonic vibrations reduce the effective friction force up to 62%. Consistent with previous studies, the benefit of ultrasonic vibrations diminishes with increasing speed, though 29% friction force reduction was still achieved at 87 mm s^{-1}. Other parameters such as contact

Table 6. Comparison of model and test results of wear reduction.

Linear speed (m s^{-1})	Wear rate ($\times 10^{-2}$ mm^3 m^{-1})					
	With US			Without US		
	Test	Model	Error	Test	Model	Error
20.3	2.237	2.566	14.7%	1.214	1.335	11.6%
40.6	2.581	2.566	0.58%	1.338	1.335	1.27%
87	2.430	2.566	5.6%	1.248	1.335	8.57%

stiffness, surface roughness, and materials hardness are known to participate in ultrasonic lubrication. Those parameters will be the subject of a future study. Further, characterization of ultrasonic lubrication will be performed at higher speeds and normal pressures. According to theory, higher ultrasonic power is required to achieve the same degree of ultrasonic lubrication achieved at lower speeds and pressures.

The wear measurements show a consistent reduction in volume loss of up to 49%, with little dependency on velocity at the speeds considered. A slight increase in the effectiveness of wear reduction at 87 mm s^{-1} is attributed to a decrease in the number of contacts over the duration of the test. The SEM images of wear grooves show abrasive mode with small scale features located 3.6 μm apart that appear to be created by a punching action of the pin as it vibrates at 22 kHz over the surface of the disc. Larger scale indentations located approximately 0.9 mm apart appear to be created by stick-slip at a frequency of approximately 100 Hz. The measurements show that stick-slip amplitudes decrease up to 61% when ultrasonic vibrations are applied. However, no clear trend is found in the relationship between stick-slip reduction and linear speeds. Future work will focus on the relationship between system stiffness and stick-slip amplitudes.

A simple cube model previously developed to quantify friction force reduction was implemented to describe the wear measurements conducted in this study. Without fundamental modifications, the model describes wear reduction within 15% of the experimental data.

Acknowledgments

The authors would like to acknowledge Tim Krantz from NASA Glenn Research Centre and Duane Detwiler from Honda R & D Americas for their technical support and in-kind contributions. Financial support for this research was provided by the member organizations of the Smart Vehicle Concepts Center (www.SmartVehicleCenter.org), a National Science Foundation Industry/University Cooperative Research Center (I/UCRC). SD is supported by a Smart Vehicle Concepts Graduate Fellowship.

References

[1] Bhushan B 2002 *Introduction to tribology* (New York: Wiley)
[2] Uchino K 1998 Piezoelectric ultrasonic motors overview *Smart. Mater. Struct.* **7** 273–85
[3] Atherton M, Mares C and Stolarski T 2014 Some fundamental aspects of self-levitating sliding contact bearings and their practical implementations *Proc. Inst. Mech. Eng. J: J. Eng. Tribol.* **0** 1–12
[4] Severdenko V, Klubovich V and Stepanenko A 1972 *Ultrasonic Rolling and Drawing of Metals* (New York: Consultants Bureau)
[5] Pohlman R and Lehfeldt E 1966 Influence of ultrasonic vibration on metallic friction *Ultrasonics* **4** 178–85
[6] Littmann W, Storck H and Wallaschek J 2001 Sliding friction in the presence of ultrasonic oscillations: superposition of longitudinal oscillations *Arch. Appl. Mech.* **71** 549–54
[7] Littmann W, Storck H and Wallaschek J 2001 Reduction in friction using piezoelectrically excited ultrasonic vibrations *Proc. SPIE* **4331** 302–11
[8] Bharadwaj S and Dapino M 2010 Friction control in automotive seat belt systems by piezoelectrically generated ultrasonic vibrations *Proc. SPIE* **7645** 76450E
[9] Bharadwaj S and Dapino M 2009 Effect of load on active friction control using ultrasonic vibrations *Proc. SPIE* **7290** 72900G
[10] Kumar V and Hutchings I 2004 Reduction of the sliding friction of metals by the application of longitudinal or transverse ultrasonic vibration *Tribol. Int.* **37** 833–40
[11] Popov V, Starcevic J and Filippov A 2010 Influence of ultrasonic in-plane oscillations on static and sliding friction and intrinsic length scale of dry friction processes *Tribol. Lett.* **39** 25–30
[12] Dong S and Dapino M 2012 Piezoelectrically-induced ultrasonic lubrication by way of Poisson effect *Proc. SPIE* **8343** 83430L
[13] Dong S and Dapino M 2014 Elastic-plastic cube model for ultrasonic friction reduction via Poisson effect *Ultrasonics* **54** 343–50
[14] Chowdhury M and Helali M 2007 The effect of frequency of vibration and humidity on the wear rate *Wear* **262** 198–203
[15] Bryant M, Tewari A and York D 1998 Effect of micro (rocking) vibrations and surface waviness on wear and wear debris *Wear* **216** 60–69
[16] Bryant M and York D 2000 Measurements and correlations of slider vibrations and wear *J. Tribol.* **122** 374–80
[17] Goto H, Ashida M and Terauchi Y 1984 Effect of ultrasonic vibration on the wear characteristics of a carbon steel: analysis of the wear mechanism *Wear* **94** 13–27
[18] Goto H, Ashida M and Terauchi Y 1986 Wear behaviour of a carbon steel subjected to an ultrasonic vibration effect superimposed on a static contact load *Wear* **110** 169–81

[19] ASTM G99-95 1995 Standard test method for wear testing with a pin on disc apparatus (West Conshohocken: ASTM International)
[20] Robinowicz E 1965 *The Friction and Wear of Materials* (New York: Wiley) pp 94–101
[21] Bowden F and Freitag E 1985 The friction of solids at very high speeds *Proc. R. Soc.* A **248** 350–67
[22] Burwell J and Rabinowicz E 1953 The nature of the coefficient of friction *J. Appl. Phys.* **24** 136–9
[23] Cocks M 1962 Interaction of sliding metal surfaces *J. Appl. Phys.* **33** 2152–61
[24] Goddard J and Wilman M 1962 A theory of friction and wear during the abrasion of metals *Wear* **5** 114–35
[25] Mulhearn T and Samuels L 1962 The abrasion of metals: a model of the process *Wear* **5** 478–98
[26] Sampson J, Morgan F, Reed D and Muskat M 1943 Friction behavior during the slip portion of the stick-slip process *J. Appl. Phys.* **14** 689–700
[27] Shi X and Polycarpou A 2005 Measurement and modeling of normal contact stiffness and contact damping at the meso scale *J. Tribol.* **127** 52–60